

to produce tadpoles. Based on larval (Sokol, 1959, 1962, 1977; Rabb and Rabb, 1963) and adult (Boulenger, 1899; Noble, 1924; Haas, 1961; Perret, 1966) characters, these individuals were identified as *H. boettgeri*.

Frog Maintenance and Mating

Hymenochirus are kept in 10-liter tanks of double carbon-filtered tap water in a 26°C room, 6 to 12 to a tank, separated by sex. For mating, 1 male and 1 female are placed together in a separate tank, and 0.06 ml (500 IU/ml) of human chorionic gonadotropin (Sigma) is injected into the dorsal lymph sac of each. Frogs usually amplex and the female begins laying eggs after about 10 hr, laying as many as 1500 eggs over a several-hour period. Eggs are 0.75 mm in diameter without their jelly coats. Embryos are dejellied by rinsing in a solution of 2% cysteine and 0.1% bovine serum albumin (BSA) adjusted to pH 8.0 and then washing in 33% modified Barth's solution (MBS: Gurdon, 1977) plus 0.1% BSA. Dejellying and all subsequent procedures were performed at room temperature.

Embryo Staging

No staging table is available for *Hymenochirus*, but the standard staging table for *Xenopus* (Nieuwkoop and Faber, 1967) is adequate for the stages considered here (through early tailbud). Though the shape of the blastopore in the early gastrula differs (Minsuk, 1992, 1995), gastrula stages could be identified according to the angle of arc through which the bottle cell pigment line and blastopore lip formation had progressed. In neurula and tailbud stages, the anus moves ventrally and the tailbud begins to form comparatively early; staging was entirely by the progression of neural fold formation and fusion and the development of head structures.

Scanning Electron Microscopy (SEM)

SEM was done as previously described (Keller and Danilchik, 1988) with the addition of postfixation in 1% OsO₄ in 1 M sodium cacodylate buffer, pH 7.4, for at least an hour, prior to fracturing.

Embryo Labeling

Embryos were labeled with 70- or 10-kDa, lysine-fixable fluorescein-conjugated dextran amine (Molecular Probes; Gimlich and Braun, 1985). Embryos at the 1-, 2-, and 4-cell stages were placed in 100% MBS plus 0.1% BSA and 5% Ficoll. Label was air pressure-injected into all blastomeres of each embryo using a micropipet needle mounted on a micromanipulator, similar to the method previously described (Keller and Tibbetts, 1989). After about 1 hr, embryos were transferred into 33% MBS plus 0.1% BSA and 5% Ficoll.

Marginal Zone Grafts

Grafts were made from fluorescently labeled donor embryos into unlabeled host embryos of the same stage. Dorsal grafts were done between stages 10 and 10.25 and lateral grafts between 10+ and 10.5. Embryos were transferred into Winklbauer's dissociation medium (Winklbauer, 1988), a Ca²⁺/Mg²⁺-free buffered saline, to facilitate the clean removal of epithelial tissue with a minimum of attached deep mesenchymal cells. An eyebrow-hair knife was used to gently tease back and remove the dorsal (DMZ) or lateral (LMZ)

marginal zone epithelium from the host (Figs. 1A and 1B); the remaining embryo was transferred immediately into Sater modified Danilchik's solution (Sater *et al.*, 1994) plus 0.1% BSA. A similarly sized piece of epithelium from the same position was then removed from the labeled donor embryo, taking special care to remove all adhering deep cells, and the explanted epithelium was gently placed onto the exposed mesenchymal region of the host in its normal orientation. The grafted embryos were then allowed to heal and gastrulate in the dark. Around the end of gastrulation (stage 13–14), embryos to be cultured for a longer time were transferred into 33% MBS plus 0.1% BSA.

Time-Lapse Video Micrography

To expose the archenteron roof to the camera, embryos were "fileted" at stage 14–16 by inserting an eyebrow-hair knife into the blastopore, through the archenteron and out through the anterior tip of the embryo, and then slitting all the way through the ventral side along the midline (Fig. 1C). The filet was then placed face down in 100% MBS plus 0.1% BSA in a dish with a coverslip bottom and held loosely in place by another fragment of coverslip supported by silicone vacuum grease at both ends. After 15–45 min to allow for healing, the 100% MBS plus 0.1% BSA was replaced with 33% MBS plus 0.1% BSA. The embryo was then placed on an inverted Nikon microscope and viewed under low light with epifluorescence, and images were recorded with a Hamamatsu SIT camera, Image 1 image processing software (Universal Imaging Corp.), and a Panasonic optical memory disk recorder.

Fixation and Histology

Specimens were fixed in MEMFA (0.1 M Mops, pH 7.4, 2 mM EGTA, 1 mM MgSO₄, 3.7% formaldehyde), dehydrated through an ethanol series or transferred directly into 100% ethanol, cleared in Histosol, embedded in Paraplast, and sectioned at 10 µm.

RESULTS

Lineage Tracing of Archenteron Roof Superficial Cells Reveals Their Mesodermal Fate

In order to demonstrate the movement of superficial cells to the deep layer and their mesodermal fate, we grafted superficial tissue from fluorescently labeled donors into unlabeled hosts as described under Materials and Methods. This enabled us to map the fates of the labeled cells and to follow their movements with time-lapse video micrography (see below).

Most of the grafted embryos (82%) developed normally; abnormal embryos were discarded. Embryos were fixed and sectioned at various stages to reveal the location of labeled cells. The earliest fixed embryos served as a control demonstrating that no labeled deep cells had been transferred with the grafted tissue.

Embryos were scored as either negative or positive for the presence of label in the notochord, and similarly for the somitic mesoderm. Controls had 0–5 labeled deep cells in each embryo; this established the threshold below which controls and experimental embryos were scored as negative. Embryos scored as positive usually had at least 20 labeled

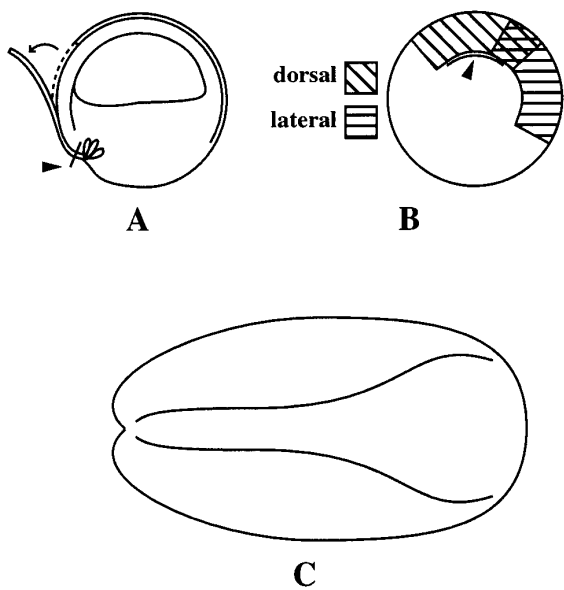


FIG. 1. (A, B) Marginal zone epithelial grafts. (A) Cutaway sagittal view of stage 10 embryo, with DMZ epithelium being removed (arrow). Dorsal is left. Pointer indicates location of vegetal cut. (B) Vegetal view. Pointer indicates dorsal blastopore lip. Hatched areas indicate locations of DMZ and LMZ grafts. (C) A "fileted" early neurula (viewed from ectodermal side, showing outline of neural plate), anterior right. Entire perimeter represents the ventral midline of the embryo.

cells that could be counted in the tissue in question (notochord or somite), making this all-or-none scoring possible.

Dorsal grafts. Twenty-three dorsal grafts (Figs. 1A and 1B) were fixed at late gastrula to mid tailbud stages and analyzed (Table 1). Histological sections show that all grafted, labeled tissue was still superficial at stages 12–14 (Figs. 2A and 2B), demonstrating that no deep cells were transferred with the grafted tissue and that no non-stage-specific invasion of the deep layer occurs prior to stage 15.

Labeled cells at stages 15–19 (Figs. 2C–2E) populated the notochord and somites (Table 1), and by stages 22–25 (Figs. 2F–2G), they show normal morphological differentiation. Labeled cells in the notochord (Figs. 2D, 2F, and 2G) show the "stack of pizza slices" morphology typical of notochord cells and are scattered among unlabeled cells as expected of normal mediolaterally intercalating tissue (Keller *et al.*, 1989). Labeled cells in the somite, on the other hand, are elongated along the anterior–posterior (A–P) axis. Grafted epithelial cells therefore are capable of leaving the superficial archenteron lining to become an integrated part of the deep mesodermal structures.

The fact that the controls (Figs. 2A and 2B) were analyzed as late as stage 14, at least 7 hr after the grafting procedure, demonstrates that the appearance of label in the deep cells at stage 15 (Figs. 2C–2E) occurs rapidly and only after a considerable delay. Therefore, it cannot be explained as the subsequent proliferation of an initial few stray labeled deep

cells; labeled cells appearing in the deep layer originate in the epithelium, invading the deep layer in a stage-specific manner.

Lateral grafts. In addition to dorsal grafts, five lateral grafts were analyzed (Figs. 1A and 1B, Table 1). These behaved similarly to the dorsal grafts. In the early neurula, fluorescent tissue ended up in the dorsolateral archenteron roof epithelium and the dorsolateral superficial layer of the ectoderm, with no label visible in the deep layers. In the later (tailbud) stages, labeled cells appeared in the somites in all embryos, but in only one case did they appear in the notochord. Labeled cells that remained in the epithelium occupied a strip at or near the midline. The lateral grafts have therefore undergone a large amount of convergence toward the midline, occupying a final dorsal–ventral position largely overlapping that of the dorsal grafts. These data confirm the stage-specific nature of the cell movement into the deep layer. Furthermore, they suggest that the final location of labeled mesoderm cells (in notochord or in somite) reflects their site of origin in the roof epithelium (mid dorsal or dorsolateral) and that presumptive endoderm lateral to the invading cells moves dorsally to fuse with the contralateral endoderm at the midline, as the invading cells leave the surface.

Surface Area Shrinks as Surface Cells Invade the Deep Layer

Fluorescent DMZ epithelial grafts were performed as above, and embryos were "fileted" at the early neurula stage to expose the archenteron roof for time-lapse video microscopy (see Materials and Methods). Labeled superficial cells are bright and easy to focus, while labeled cells in the deep layer must be viewed through the epithelium, so they are dim and cannot be focused sharply. Therefore, the bright area of the filet represents the grafted cells still remaining in the surface.

The shrinking surface area of the label (Fig. 3) reveals the removal of cells from the surface as they invade the deep layer. The embryo pictured was fileted at stage 14 (early neurula). The labeled area remained static until 3 hr later (Fig. 3A), when it started to shrink. It continued shrinking

TABLE 1
Epithelial Grafting Experiments

Type of graft	Total number	Stage (N)	Labeled notochord ^a	Labeled somite ^a
Dorsal	23	12–14 (7)	0	0
		15–19 (8)	6	6
		22–25 (8)	7	5
Lateral	5	14 (1)	0	0
		22–30 (4)	1	4

^a Number of grafted embryos scored positive for the presence of labeled cells in these tissues.

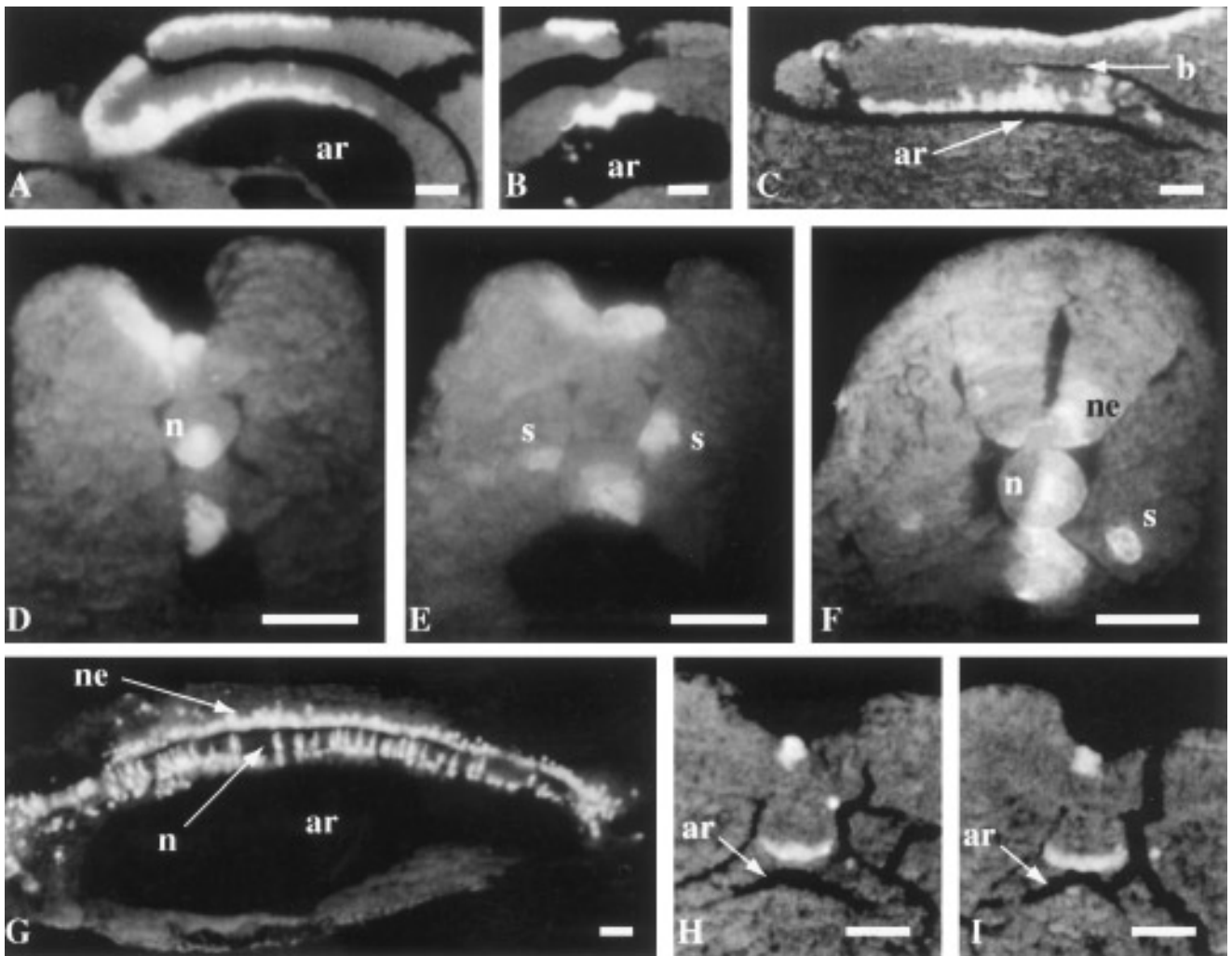


FIG. 2. Epifluorescent images of sections of DMZ grafted embryos after development to various stages. (A, C, G) sagittal sections; all others, transverse sections; dorsal is up in all photos. (A, B) Late gastrulae (stages 12 and 13, respectively); only the superficial layer is labeled; ar, archenteron. (C–E) Mid neurulae (stage 16); deep layer is labeled. (C) While uninvoluted label remains superficial, involuted label now spans the deep and superficial layers, from the lining of the archenteron to the boundary (b) between the involuted and uninvoluted regions. (D) Labeled cells can be found in the notochord (n). (E) In another section of the same embryo, labeled cells can be found in the somites (s). (F, G) Tailbud stage embryos; labeled notochord and somite cells differentiate normally. Cells in the notochord are flat discs oriented perpendicular to the A-P axis. Somite cell in (F) shows much smaller cross-sectional area, due to its elongation and alignment parallel to the axis; ne, labeled neural tissue, now at the ventral midline of the neural tube. (H, I) Two sections from one stage 15 embryo show crescent-shaped cells adhering to the ventral notochord. The cell in (H) has no apex exposed to the lumen of the archenteron, but neither does it have typical notochord cell shape. The cell in (I) is very similar but still has a luminal apex. Compare to Fig. 6B. Bars: 50 μ m.

until 11 hr (Fig. 3C) and then stopped; no additional loss of surface label occurred before the video recording was stopped at 21 hr.

SEM Reveals Novel Morphology of the Archenteron Roof and Mesoderm

We examined normal unoperated embryos with SEM and observed the archenteron roof and the underlying dorsal

axial structures. Throughout gastrulation, the roof epithelium is morphologically undifferentiated and distinct from the deep layer (not shown), just as in *Xenopus*. From stage 15 (early neural folds) until at least stage 19 (initial neural fold contact), the roof displays novel morphological features reflecting the movement of cells from the surface into the deep layer and suggesting the nature of the cellular mechanisms of these movements.

The mid to late neurula roof consists of three distinct

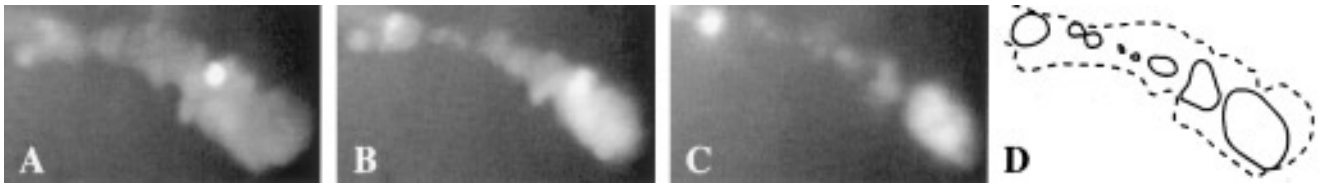


FIG. 3. (A–C) Three time points in a video recording of the archenteron roof of a fileted embryo that received a DMZ fluorescent epithelial graft in the early gastrula. The embryo was fileted at stage 14 (early neurula). Anterior is right. The region shown is the mid trunk region, and the long axis of the fluorescent area is the dorsal midline. (A) 3 hr after fileting; (B) 6 hr; (C) 11 hr. (D) Tracings of (A) and (C) superimposed to show the reduction in area.

longitudinal zones: two lateral zones separated by a midline zone. The edges of each zone are indicated by sharp morphological boundaries (Fig. 4A). The apical surfaces of the cells within the lateral zones appear flatter than those elsewhere. These zones extend along the posterior half of the embryo (Fig. 4A), narrowing from an initial width of about four cells at stage 15 down to only one cell before finally disappearing at the late neurula stage.

Fractures through the dorsal axis reveal that the cells within the lateral zones belong to the paraxial or somitic mesoderm and form its ventral surface, which is exposed to the lumen of the archenteron (Figs. 4B and 4C). We refer to these zones of luminal somitic epithelial cells as the paraxial zones. These cells are well integrated into the somite structure (Figs. 4B and 4C), yet share the epithelial character of the surface layer, as indicated by the tightly sealed margins of the cells (Figs. 4A, 4C, and 5). Outside these zones, the epithelium of the archenteron wall is independent of the deep layer (Fig. 4B) and constitutes the lateral endodermal crests (Vogt, 1929). The paraxial zone cells are continuous with the endodermal crests (Fig. 5A) as well as with the medial zone cells and are therefore simultaneously part of the somite and part of the epithelial lining of the archenteron. Histological sections (not shown) confirm the novel morphology seen in SEM. This morphology suggests that the paraxial zone cells are in the process of moving from one layer to the other (though it does not logically indicate which tissue is their source and which is their destination). Taken together with the results of our grafting and video recording experiments, this strongly suggests they are moving from the roof epithelium into the deep, mesenchymal somitic mesoderm.

In some specimens, the endodermal crests and the somitic mesoderm fortuitously separated from each other during fracturing. In these cases, the paraxial zone cells always stayed integrated with the somite, probably due to the greater contact they share with other somitic cells than with the neighboring endodermal cells. These epithelial cells are distinguishable from the mesenchymal cells within the somites by their different size, shape, and surface morphology (Figs. 4C and 5). Their distinct morphology, along with their structural integration with the somitic mesoderm, further support the conclusion that they have an independent, epithelial origin and are in the process of becoming deep and somitic.

Along the dorsal midline, between the bilateral paraxial zones, lies a strip of epithelial cells which we refer to as the axial zone. Some of these cells appear to be in the process of leaving the surface to join the notochord, but they display a morphology different from that of the paraxial zone cells joining the somites. Individual cells scattered along the exact midline of the roof appear much smaller than their immediate neighbors in a surface view (Fig. 4A). Fractures through the dorsal axis (Fig. 6A) reveal that these cells are as large as their neighbors; only their apical surfaces are reduced, most of the cell body being hidden from the surface. These cells are spread out over the deep cells of the notochord, extending lamellipodia laterally from their basal ends (Fig. 6). In contrast to the flattening of the apical surfaces in the paraxial zone, these cells bulge outward into the archenteron lumen (Figs. 4A and 6). The remaining axial zone cells are situated lateral to these midline cells but medial to the paraxial zones (Fig. 6A). They have typical epithelial morphology and have little if any contact with deep notochordal cells. They may leave the surface at a later time, or they may remain in the surface and differentiate as endoderm.

In the further developed anterior trunk region of a stage 15 embryo, where the notochord has already taken on a cylindrical shape and the individual cells have begun to take on their characteristic pizza-slice geometry (Fig. 6B), the invasion of the notochord by midline axial zone cells is also more advanced. Some cells have the same geometry as more posterior ones (Fig. 6B, solid arrow), with small constricted apices exposed to the lumen while their basal ends are spread on the notochord. Other cells, however, are similarly spread on the ventral notochord surface, but without any luminal apex (Fig. 6B, open arrows). These cells seem to be within the cylindrical outline of the notochord, but they have not taken on pizza-slice morphology as have the other notochord cells, instead sitting as crescents on the ventral surface. This suggests that individual axial zone cells have recently ingressed from the surface to become deep cells and are in a transient state prior to taking on typical notochord cell morphology; crescent-shaped cells are not seen in this position at later stages (data not shown).

Similar crescent-shaped ventral notochord cells can occasionally be seen in fluorescently grafted embryos of the same stage. Like those seen in SEM, these cells may be completely deep, separated from the archenteron lumen by

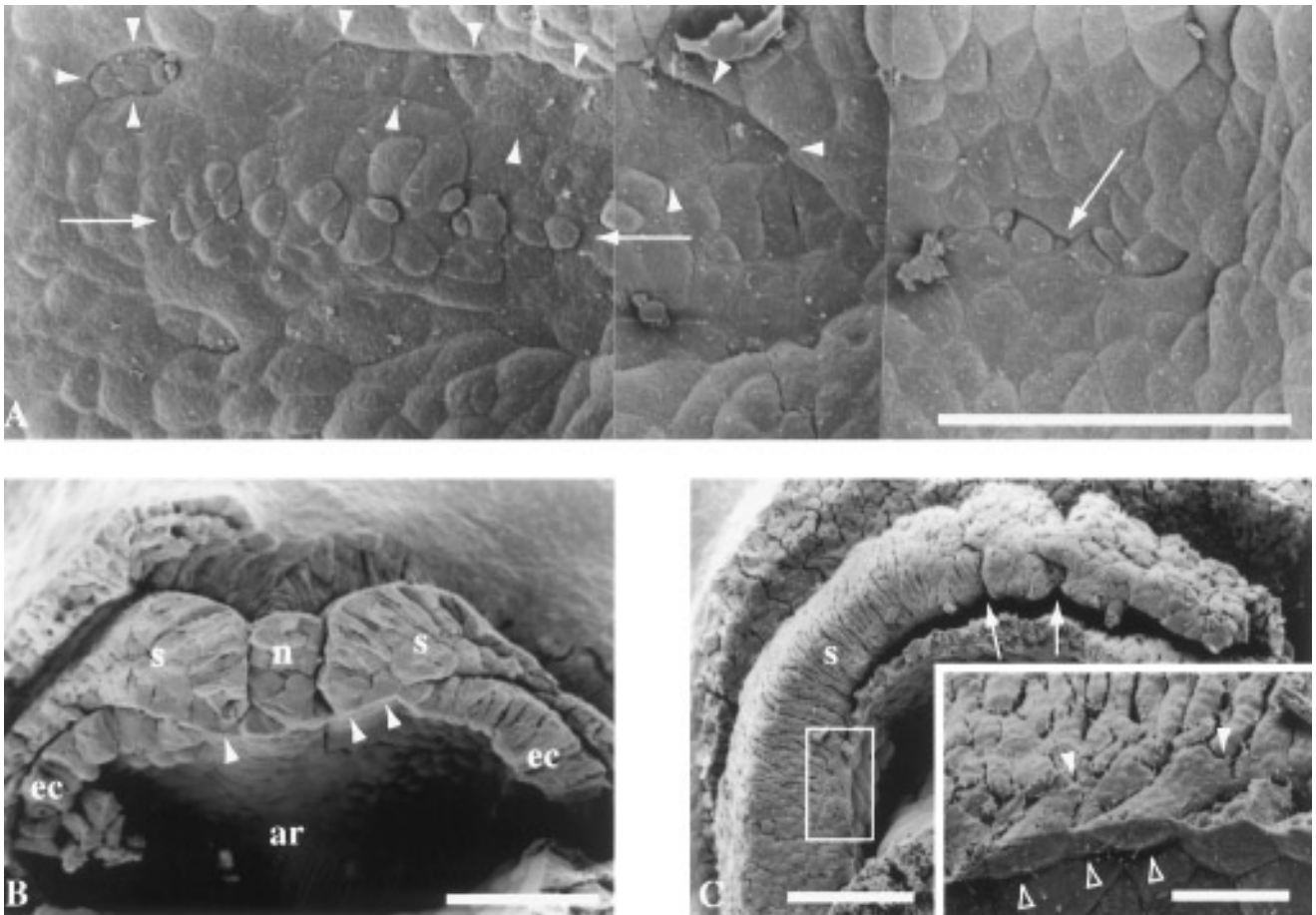


FIG. 4. SEM of mid to late neurulae. (A) Surface of the archenteron roof epithelium, viewed from inside the archenteron at stage 18. Anterior is right, and the dorsal midline runs horizontally through the center of the field. On each side of the dorsal midline lies a zone of cells sharply delimited from its neighbors by visible boundaries. (Pointers indicate one of the two zones.) Along the exact dorsal midline lies a row of cells (arrows) having smaller cell apices than their neighbors. (B) Transverse fracture through the posterior dorsal axis at stage 15. Pointers indicate the cells of the paraxial zones; ec, endodermal crests. (C) A parasagittal fracture at stage 19 removed the right side of the embryo including the notochord, revealing the somitic mesoderm, which is just beginning to segment anteriorly (arrows). The surface layer is independent from the somitic mesoderm along most of its length, except in the posterior region (box). Inset is a closeup of the boxed region. The basal ends of the surface cells interact closely with the deep cells (solid pointers), while their apical surfaces are integrated into the epithelium. The zone is only one cell wide and quite narrow; open pointers indicate its lateral boundary. Bars: A–C, 100 μ m; C, inset, 25 μ m.

intervening superficial cells (Fig. 2H), or they may bulge centrally out into the lumen (Fig. 2I).

By stage 20, the superficial and deep layers (definitive endoderm, and mesoderm, respectively) are once again distinct. The superficial layer is homogeneous with no hint of special zones, just as in *X. laevis*.

DISCUSSION

The present study demonstrates that *Hymenochirus*, unlike its close relative, *X. laevis*, has surface layer contributions to both notochord and somite. Furthermore, the invasion of the deep layer by surface cells involves novel mor-

phogenetic mechanisms that raise important issues for the understanding of mesoderm morphogenesis and its evolution.

Xenopus Is Unusual in Lacking Surface Mesoderm

Early histological work on amphibian mesoderm morphogenesis (reviewed in Brachet, 1902, and King, 1903; also Goodale, 1911; Ruffini, 1925) established that the surface layer of the involuted material contributes to mesoderm in all of the urodeles studied, but opinion was divided on whether this was also the case in anurans. Later, true fate mapping studies using vital dyes consistently found surface mesoderm in additional, previously unstudied species, both

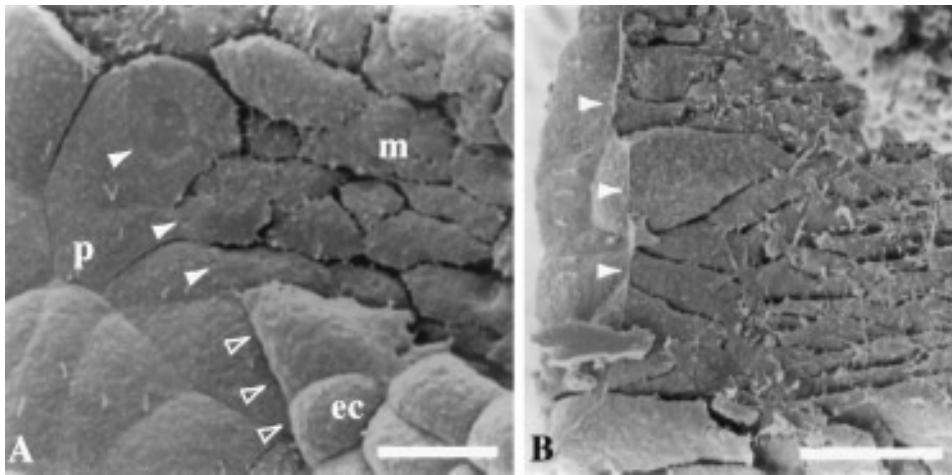


FIG. 5. Anterior is up, medial is left in both figures. (A) Stage 15 embryo in which part of the endodermal crest (ec) has been removed, revealing the basolateral surfaces of the paraxial zone (p) cells as well as the remaining, mesenchymal (m), somitic deep cells. Note the difference in size and shape between the cells of the two populations. The fracture separated the crest cleanly from the paraxial epithelium, revealing a sharp edge bounding the apical and basolateral surfaces of the paraxial zone cells (solid pointers). This edge is coincident with the boundary between the paraxial zone and the endodermal crest (open pointers). (B) Isolated, intact somite from a stage 19 embryo, viewed from its ventral surface. The cells on the left are epithelial and their apical surfaces represent the full 1- to 2-cell width of the surface paraxial zone. Pointers indicate the apical/basolateral boundary where the endodermal crest had been joined. The surface cells are well integrated with the deep mesenchymal cells (right), but are larger, less flattened, and lack the extensive network of filopodia and lamellipodia of the deep cells. Bars: 25 μ m.

urodele (Vogt, 1929; Nakamura, 1938; Pasteels, 1942) and anuran (Vogt, 1929; Wintrebert, 1930; Pasteels, 1942). *X. laevis* turns out to be an exception, forming its mesoderm entirely from the involuted deep cells, while the involuted superficial layer forms the endodermal lining of the archenteron (Nieuwkoop and Florschütz, 1950; Keller, 1975). This led to the overgeneralization that the *X. laevis* results were applicable to all anurans (Nieuwkoop and Sutasurya, 1976) or even to all amphibians (Løvtrup, 1965, 1966, 1975). With the ascendance of this species as the predominant model system for amphibian development, the existence of surface mesoderm and its morphogenetic mechanism became a nonissue. It was pointed out, however, that results in *X. laevis* could not be assumed to apply to other species without further evidence, and it was predicted that greater diversity would be found in amphibian gastrulation mechanisms than is commonly acknowledged to exist (Keller, 1976). Modern studies have borne out this prediction, revealing the presence of surface mesoderm in several anurans (Purcell, 1992; Purcell and Keller, 1993; Delarue *et al.*, 1994) as well as in urodeles (Löffberg, 1974; Smith and Malacinski, 1983; Brun and Garson, 1984; Lundmark, 1986; Delarue *et al.*, 1992). We see the diversity of mesoderm morphogenesis as an opportunity for alternative approaches to issues of morphogenetic mechanism and its evolution.

Hymenochirus Has Surface Mesoderm

Hymenochirus archenteron roof morphology suggests the movement of surface cells into the notochord and somites,

as has been demonstrated in other anurans. Grafting experiments support this hypothesis. Grafted cells invade the notochord and somites and develop normally, indicating active participation in tissue differentiation; nonparticipating cells placed within developing notochord do not just get passively squashed into normal notochord cell shape, but are squeezed out of the structure (Domingo and Keller, 1995).

There is a rough correlation between the graft location and the final position of the labeled mesoderm. Dorsal grafts contribute significantly to both notochord and somite, while lateral grafts contribute mostly to somite. This suggests that invasion of the mesoderm is local, without long-distance migration of cells mediolaterally once they join the deep layer. This is consistent with the two separate populations of invading cells observed in SEM, an axial population that invades the notochord, and bilaterally paired paraxial populations that invade the somites (Fig. 7).

The behavior of grafted cells does not directly prove that normal endogenous cells behave the same way. However, invasion of the deep layer is stage-specific, with the cells remaining superficial through stage 14, after grafting at stage 10 to 10.5. If the invasive behavior were abnormal, due to the experimental manipulation, it would most likely occur immediately after grafting. Furthermore, the morphological features seen in intact embryos in SEM appear at stage 15, exactly coinciding with the timing of the invasion tracked in the grafting experiments. These facts convince us that the invasive activity represents the normal endogenous activity of archenteron roof cells.

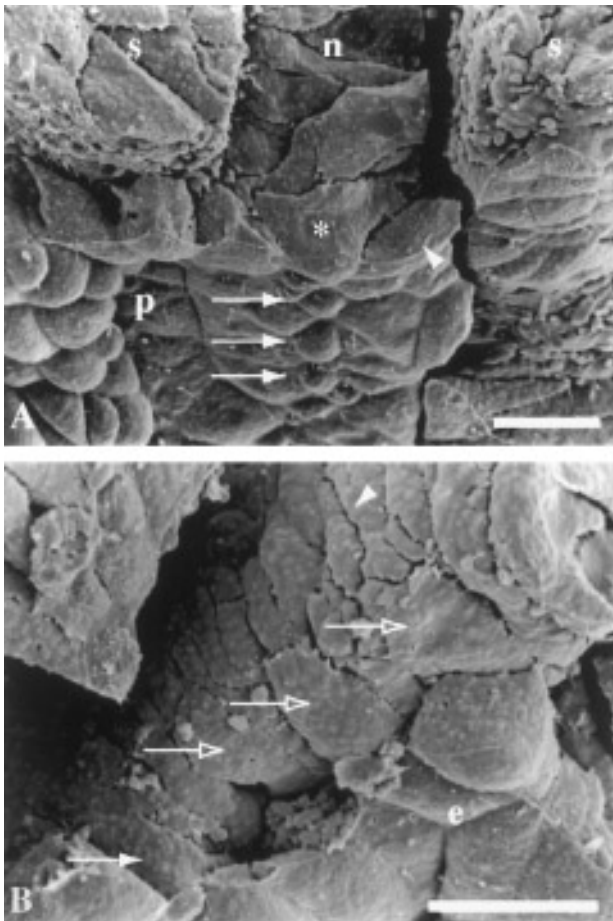


FIG. 6. Stage 15 notochord and the associated axial zone of the surface layer. (A) Posterior transverse fracture revealing midline surface cell (asterisk). This cell is one of a row of midline cells with small apical surface area (arrows), but its base is large and spread over most of the width of the notochord (n). Non-midline axial zone cells (pointer) have typical epithelial morphology; s, somites; p, paraxial zone. (B) Anterior notochord at the same stage. In this region the notochord has become cylindrical and most of the cells are flattened (pointer). Solid arrow indicates a cell that is spread on the ventral notochord surface, with a small luminal apex, similar to those in (A). Open arrows indicate crescent-shaped deep cells without luminal apices, but also without the typical flattened notochord cell shape. Compare to Figs. 2H and 2I; e, epithelial layer. Bars: 25 μ m.

Cellular Mechanisms of Mesoderm Invasion

How do surface cells find their way into the deep layer? Early observations (Brachet, 1902; King, 1903; Vogt, 1929) were consistent with the formation of a gap in the surface layer as the presumptive mesoderm separates from the definitive endodermal regions (the "lateral endodermal crests"; Vogt, 1929; Brun and Garson, 1984). But modern studies (in different species) showed instead an alternative mechanism, the individual ingression of cells without any rupture in the surface layer (Holtfreter, 1943; Purcell, 1992;

Purcell and Keller, 1993; Delarue *et al.*, 1994). Our results suggest that *Hymenochirus* uses both strategies, one in the paraxial and one in the axial zone.

In the paraxial zones, superficial cells appear to change their relationships to neighboring tissues *en masse* (Figs. 7A and 7B). Within the boundaries of each zone, all the cells develop an affinity for the deep somitic cells and adhere to those deep cells, integrating into the structure of the somites even while they retain their epithelial properties, remaining tightly attached to one another at their apical surfaces (Fig. 7B). This mechanism of moving presumptive mesoderm cells from the surface to the deep layer has not previously been described for other amphibians. It is distinct from the familiar morphogenetic processes such as ingression, invagination, and involution and requires a new name. We dub this process "relamination." (We use "invasion" as a general umbrella term to indicate movement of cells from superficial to deep without reference to the mechanism, be it relamination, ingression, or some other alternative.)

Subsequent to this rearrangement the paraxial zones narrow, accompanied by the movement of the lateral endodermal crests to the dorsal midline, where they fuse, closing up the gap between them and recreating a smooth, intact epithelium (Figs. 7B–7D). The relaminated cells end up deep and mesenchymal (Figs. 7D and 7D'). Individual cells in the paraxial zones lack rounded, constricted apices (Fig. 4A), but they do narrow mediolaterally (Fig. 4C, inset), suggesting that they secondarily undergo a progressive removal (or transformation) of apical membrane inward from the medial and/or the lateral boundaries, until their apical surfaces are eliminated and the cells dissociate from the neighboring epithelia (Figs. 7B–7D). Since the leading edges of the crests are always associated with the most lateral extent of the apical surfaces of the narrowing paraxial zones (Figs. 4B, 5A, 7B, and 7C), the crests do not have truly free, migrating edges. The forces driving dorsal convergence of the crests are unknown, but they must be tightly coupled to the progressive loss of epithelial character by the new somite cells of the paraxial zones.

In the axial zone, surface mesoderm cells invade the deep layer by a mechanism distinct from that of the paraxial zones (Fig. 7). Individual cells leave the surface one at a time. Their apical surfaces shrink and ultimately release their connection to neighboring cells. Though this constitutes ingression, the mechanism at the cellular level appears to be different from that proposed for apically constricting archenteron roof cells in other species. In *Hymenochirus*, these cells spread their basal ends over the surface of the deep notochord cells (Figs. 6 and 7), suggesting that the ingressing cells actively crawl, pulling themselves out of the epithelium. In contrast, surface-derived notochord cells in other amphibians (Löffberg, 1974; Purcell, 1992; Purcell and Keller, 1993), as well as in sturgeon (Bolker, 1993), are elongated in the apical–basal axis, with rounded basal ends (Fig. 8, top). This morphology is similar to that of the bottle cells of the blastopore lip, suggesting that their elongation is passive, dependent upon active constriction

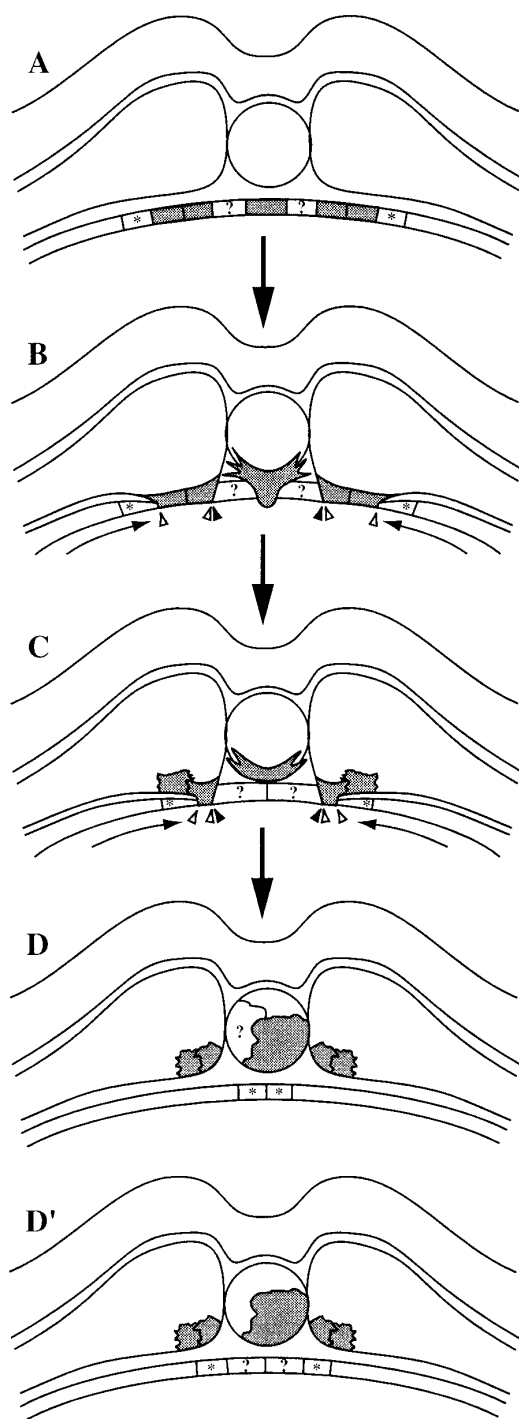


FIG. 7. Mechanism of surface mesoderm morphogenesis in *Hymenochirus*. See text for full description. Shaded cells are surface mesoderm, originating in the superficial layer (A) and ultimately contributing to notochord and somite (D, D'). Solid pointers (B, C) indicate the morphological boundaries of the axial zone, and open pointers, those of the paraxial zones. Asterisks indicate cells at the leading edge of the endodermal crests, which start laterally and then converge toward the dorsal midline (arrows in B, C). Question marks indicate cells in the axial zones whose fate may be noto-

at their apical ends (Hardin and Keller, 1988). The active crawling of *Hymenochirus* surface notochord cells may be sufficient to cause ingression without such active, force-generating apical constriction.

Immediately after ingressing, some cells adhere to the ventral surface of the notochord as crescents (Fig. 7C). This is probably a transient state for ingressed cells prior to adopting typical notochord cell morphology (Figs. 7D and 7D').

Only cells at the exact midline of the axial zone are seen ingressing (Figs. 6A and 7B). The neighboring cells must spread to take up the area the midline cells vacate (Figs. 7B and 7C, cells marked with "?"), but the ultimate fate of those neighboring cells is not known. They may subsequently ingress after taking up midline positions (Fig. 7D). But the axial zone does not narrow as the paraxial zones do (Figs. 7B and 7C), so the remaining surface cells may fuse with the endodermal crests, remain superficial, and differentiate as endoderm (Fig. 7D'). The axial zone prior to ingression (Fig. 7A) would then be a mixed population of cell fates.

The Evolution of Cellular Mechanisms

Our results suggest a model of pipid mesoderm morphogenesis and the sequence of modifications leading to current diversity (Figs. 8 and 9). Ancestral anurans probably did have surface mesoderm (Purcell, 1992; Purcell and Keller, 1993), since it occurs not only in most anurans, but also in all urodeles as well as in the chondrosteian fishes, which gastrulate in the amphibian rather than the teleost fashion (Ballard and Ginsburg, 1980; Bolker, 1993) and even in some amniotes (mouse but not chick; Sulik *et al.*, 1994). Since the genera *Hymenochirus* and *Xenopus* are sister taxa relative to the other anurans studied (Fig. 9; Duellman and Trueb, 1986; Cannatella and de Sá, 1993), and *Hymenochirus* has surface mesoderm, the most likely scenario under outgroup analysis and the criterion of parsimony (Harvey and Pagel, 1991) is that the common ancestor of these two species also had surface mesoderm; the evolutionary loss of this feature would have occurred after the split, in the lineage leading to *X. laevis*.

Among vertebrates having surface mesoderm, invasion mechanisms vary. For example, in urodeles the notochord forms by an entirely different mechanism from those considered here. The surface layer invaginates, its constricting cell apices ending up at the center of the notochord, while the endodermal crests remain attached to the notochord, fusing at the midline in a process reminiscent of neural fold fusion (Löffberg, 1974; Brun and Garson, 1984). Notochord morphogenesis in the mouse (Sulik *et al.*, 1994) bears a striking resemblance to that in urodeles, with implications

chordal (D) or endodermal (D'). Approximate stages are (A) 14, (B) 15, (C) 18, (D, D') 22, though only changes in the involuted superficial layer are shown; morphogenesis of the involuted deep layer and of the ectoderm have been omitted for simplicity.

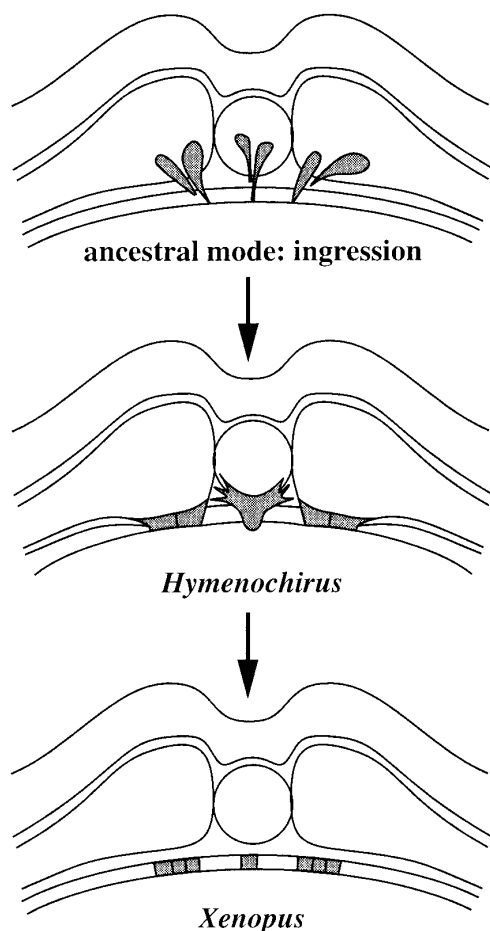


FIG. 8. A model of the different amphibian mechanisms of surface mesoderm morphogenesis and their evolutionary transformations. (Top) The ancestral mode of invasion in anurans is ingression, the individual detaching of surface cells from one another and their independent entry into both the notochord and the somitic mesoderm. (Middle) In *Hymenochirus*, surface somite cells relaminate, dissociating from the lateral endodermal crest *en masse* (without dissociating from one another) and associating instead with the somitic mesoderm. This could have arisen in a pipid ancestor by the loss of the ability of the cells to individually detach. In contrast, surface notochord cells ingress individually, but have different morphology than their homologs in other anurans, suggesting that at the subcellular level, different mechanisms are involved. (Bottom) *Xenopus* is believed not to have surface mesoderm, either in the notochord or in the somites. The relaminating surface somite of a pipid ancestor could have been subsequently transformed, in the lineage leading to *X. laevis*, by the loss of affinity for the deep cells or by the loss of the ability to interact mechanically with those cells. The superficial cells would then remain in place and differentiate as endoderm.

for the evolution of invasion mechanisms in vertebrates and for the relationship of amphibian studies to mammalian mesoderm formation.

This study has shown that even among anurans, mecha-

nisms of invasion are not universal, but can vary fundamentally among different species, and even among different regions of the embryo within a single species. Relamination in the paraxial zone of *Hymenochirus* is fundamentally different from ingression, and ingression itself is not a simple universal process, but can occur by mechanisms as different as the apically driven elongation proposed for *Ceratophrys ornata* (Purcell, 1992; Purcell and Keller, 1993) and the basolateral invasive crawling we see in the axial zone of *Hymenochirus*. An evolutionary model must account for this diversity of mechanism.

C. ornata surface mesoderm invades in distinct axial and paraxial zones similar to those in *Hymenochirus*, but in both regions invasion is by ingression (Fig. 8, top; Purcell and Keller, 1993). Ingressing surface mesoderm cells must deepithelialize and must also interact mechanically with the underlying deep cells. Surface cells in *X. laevis* have lost both behaviors: they remain epithelial, and fail to interact mechanically with the deep cells. Our results in *Hymenochirus* demonstrate that these features are dissociable: paraxial zone cells adhere to the deep cells and become structur-

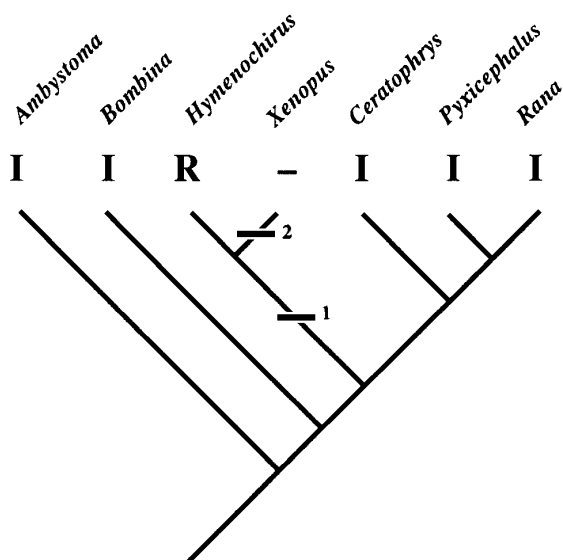


FIG. 9. Phylogenetic relationship of selected amphibians. The species shown are those that have been the subject of modern studies, and for which those studies have given evidence not only of the presence or absence of surface mesoderm, but also of its mechanism of invasion if present. *A. mexicanum*: Lundmark (1986); *B. orientalis*, *C. ornata*, *P. adspersus*: Purcell (1992), Purcell and Keller (1993); *R. pipiens*: Delarue *et al.* (1994); *X. laevis*: Nieuwkoop and Florschütz (1950), Keller (1975, 1976), Minsuk (1995), Minsuk and Keller (in preparation); *H. boettgeri*: this study and Minsuk (1995). Mechanism of invasion of the surface-derived somite cells is indicated in bold. R, relamination; I, ingression; dash, no surface mesoderm. Relationships from Duellman and Trueb (1986). Bars indicate the hypothesized course of evolutionary change in the invasion mechanism of surface somite cells (see text). Bar 1 represents the modification from ingression to relamination in a pipid ancestor. Bar 2 represents the probable loss of surface mesoderm in *X. laevis*.

ally integrated into the somites, but do so *en masse* without individually leaving the epithelium (Fig. 7B). We therefore propose that the morphogenesis of the paraxial zone by re-lamination may represent an evolutionary intermediate between the ingressing paraxial cells of *C. ornata* and the "lost" ingression of *X. laevis* (Figs. 8 and 9). If during evolution, ingressing cells (Fig. 8, top) first lost the ability to detach from their neighbors but continued to display affinity for the deep cells, they would then behave as does the *Hymenochirus* paraxial zone (Fig. 8, middle). A subsequent evolutionary loss of affinity for the deep layer could result in noninvading cells such as those in *X. laevis* (Fig. 8, bottom). This model brings order to the observed diversity and suggests testable hypotheses of morphogenetic mechanisms in these species.

ACKNOWLEDGMENTS

We thank Wendy Olson for an enjoyable collaboration in identifying our species of *Hymenochirus* and for translating portions of Vogt (1929), Lance Davidson, Carmen Domingo, Tamira Elul, John Gerhart, Wendy Olson, David Wake, and the members of his laboratory, and especially Jessica Bolker for comments on the manuscript, and the staff of the UC Berkeley Electron Microscopy Laboratory for instruction and expert advice. This work was supported by HD25594-5, NSF92-20525, 5T32 HD07375, and a UC Regents' Fellowship to S.M.

REFERENCES

- Ballard, W. W., and Ginsburg, A. S. (1980). Morphogenetic movements in Acipenserid embryos. *J. Exp. Zool.* 213, 69–103.
- Bolker, J. A. (1993). Gastrulation and mesoderm morphogenesis in the white sturgeon. *J. Exp. Zool.* 266, 116–131.
- Boulenger, G. A. (1899). On *Hymenochirus*, a new type of aglossal batrachians. *Ann. Mag. Nat. Hist. Zool. Bot. Geol.* 4, 122–125.
- Brachet, A. (1902). Recherches sur l'ontogénèse des amphibiens urodèles et anoures (*Siredon pisciformis*.—*Rana temporaria*). *Arch. Biol.* 19, 1–243.
- Brun, R. B., and Garson, J. A. (1984). Notochord formation in the Mexican salamander (*Ambystoma mexicanum*) is different from notochord formation in *Xenopus laevis*. *J. Exp. Zool.* 229, 235–240.
- Cannatella, D. C., and de Sá, R. O. (1993). *Xenopus laevis* as a model organism. *Syst. Biol.* 42, 476–507.
- Delarue, M., Johnson, K. E., and Boucaut, J.-C. (1994). Superficial cells in the early gastrula of *Rana pipiens* contribute to mesodermal derivatives. *Dev. Biol.* 165, 702–715.
- Delarue, M., Sanchez, S., Johnson, K. E., Darribère, T., and Boucaut, J.-C. (1992). A fate map of superficial and deep circumblastoporal cells in the early gastrula of *Pleurodeles waltl*. *Development* 114, 135–146.
- Domingo, C., and Keller, R. (1995). Induction of notochord cell intercalation behavior and differentiation by progressive signals in the gastrula of *Xenopus laevis*. *Development* 121, 3311–3321.
- Duellman, W. E., and Trueb, L. (1986). "Biology of Amphibians." McGraw-Hill, New York.
- Gimlich, R. L., and Braun, J. (1985). Improved fluorescent compounds for tracing cell lineage. *Dev. Biol.* 109, 509–514.
- Goodale, H. D. (1911). The early development of *Spelerpes bilineatus* (Green). *Am. J. Anat.* 12, 173–247.
- Gurdon, J. B. (1977). Methods for nuclear transplantation in amphibia. In "Methods in Cell Biology, Vol. 16, Chromatin and Chromosomal Protein Research. I," pp. 125–139. Academic Press, New York.
- Haas, R. (1961). Observations of the African frog *Hymenochirus boulengeri*. *Aquarium* 30, 620–626.
- Hardin, J., and Keller, R. (1988). The behaviour and function of bottle cells during gastrulation of *Xenopus laevis*. *Development* 103, 211–230.
- Harvey, P. H., and Pagel, M. D. (1991). "The Comparative Method in Evolutionary Biology." Oxford Univ. Press, New York.
- Holtfretey, J. (1943). A study of the mechanics of gastrulation. Part I. *J. Exp. Zool.* 94, 261–318.
- Keller, R. (1975). Vital dye mapping of the gastrula and neurula of *Xenopus laevis* I. Prospective areas and morphogenetic movements of the superficial layer. *Dev. Biol.* 42, 222–241.
- Keller, R. (1976). Vital dye mapping of the gastrula and neurula of *Xenopus laevis* II. Prospective areas and morphogenetic movements of the deep layer. *Dev. Biol.* 51, 118–137.
- Keller, R. (1986). The cellular basis of amphibian gastrulation. In "Developmental Biology: A Comprehensive Synthesis, Vol. 2, The Cellular Basis of Morphogenesis" (L. Browder, Ed.), pp. 241–327. Plenum, New York.
- Keller, R., Cooper, M. S., Danilchik, M., Tibbetts, P., and Wilson, P. A. (1989). Cell intercalation during notochord development in *Xenopus laevis*. *J. Exp. Zool.* 251, 134–154.
- Keller, R., and Danilchik, M. (1988). Regional expression, pattern and timing of convergence and extension during gastrulation of *Xenopus laevis*. *Development* 103, 193–209.
- Keller, R., and Tibbetts, P. (1989). Mediolateral cell intercalation in the dorsal, axial mesoderm of *Xenopus laevis*. *Dev. Biol.* 131, 539–549.
- King, H. D. (1903). The formation of the notochord in the amphibia. *Biol. Bull.* 4, 287–300.
- Löfberg, J. (1974). Apical surface topography of invaginating and noninvaginating cells. A scanning-transmission study of amphibian neurulae. *Dev. Biol.* 36, 311–329.
- Løvtrup, S. (1965). "Morphogenesis in the Amphibian Embryo. Gastrulation and Neurulation." Zoologica Gothoburgensia, Vol. 1. Elanders Boktryckeri Aktiebolag, Göteborg.
- Løvtrup, S. (1966). Morphogenesis in the amphibian embryo. Cell type distribution, germ layers, and fate maps. *Acta Zool.* 47, 209–276.
- Løvtrup, S. (1975). Fate maps and gastrulation in amphibia—a critique of current views. *Can. J. Zool.* 53, 473–479.
- Lundmark, C. (1986). Role of bilateral zones of ingressing superficial cells during gastrulation of *Ambystoma mexicanum*. *J. Embryol. Exp. Morphol.* 97, 47–62.
- Minsuk, S. B. (1992). Gastrulation in the frog *Hymenochirus*. *Am. Zool.* 32, 84A.
- Minsuk, S. B. (1995). "A Comparative Study of Gastrulation and Mesoderm Formation in Pipid Frogs." Ph.D. thesis, University of California, Berkeley.
- Nakamura, O. (1938). Tail formation in the urodele. *Zool. Mag.* 50, 442–446.
- Nieuwkoop, P. D., and Faber, J. (1967). "Normal Table of *Xenopus laevis* (Daudin)," 2nd ed. North-Holland, Amsterdam.
- Nieuwkoop, P. D., and Florschütz, P. A. (1950). Quelques caractères spéciaux de la gastrulation et de la neurulation de l'oeuf de *Xenopus laevis*, Daud. et de quelques autres Anoures. 1ère partie.—Etude descriptive. *Arch. Biol.* 61, 113–150.

- Nieuwkoop, P. D., and Sutasurya, L. A. (1976). Embryological evidence for a possible polyphyletic origin of the recent amphibians. *J. Embryol. Exp. Morphol.* 35, 159–167.
- Noble, G. K. (1924). Contributions to the herpetology of the Belgian Congo based on the collection of the American Museum Congo expedition, 1909–1915. Part III. Amphibia. *Bull. Am. Mus. Nat. Hist.* 49, 147–347.
- Pasteels, J. (1942). New observations concerning the maps of presumptive areas of the young amphibian gastrula. (*Amblystoma* and *Discoglossus*). *J. Exp. Zool.* 89, 255–281.
- Perret, J.-L. (1966). Les amphibiens du Cameroun. *Zool. Jb. Syst.* 93, 289–464.
- Purcell, S. M. (1992). “Pattern and Mechanism of Gastrulation and Mesoderm Morphogenesis Among Anurans.” Ph.D. thesis, University of California, Berkeley.
- Purcell, S. M., and Keller, R. (1993). A different type of amphibian mesoderm morphogenesis in *Ceratophrys ornata*. *Development* 117, 307–317.
- Rabb, G. B., and Rabb, M. S. (1963). On the behavior and breeding biology of the African pipid frog *Hymenochirus boettgeri*. *Z. Tierpsychol.* 20, 215–241.
- Ruffini, A. (1925). “Fisiogenia.” Dottor Francesco Vallardi, Milan.
- Sater, A. K., Alderton, J. M., and Steinhardt, R. A. (1994). An increase in intracellular pH during neural induction in *Xenopus*. *Development* 120, 433–442.
- Smith, J. C., and Malacinski, G. M. (1983). The origin of the mesoderm in an anuran, *Xenopus laevis*, and a urodele, *Ambystoma mexicanum*. *Dev. Biol.* 98, 250–254.
- Sokol, O. M. (1959). Studien an pipiden Fröschen I. Die Kaulquappe von *Hymenochirus curtipes* Noble. *Zool. Anz.* 162, 154–160.
- Sokol, O. M. (1962). The tadpole of *Hymenochirus boettgeri*. *Copeia* 1962(2), 272–284.
- Sokol, O. M. (1977). The free swimming *Pipa* larvae, with a review of pipid larvae and pipid phylogeny (Anura: Pipidae). *J. Morphol.* 154, 357–426.
- Sulik, K., Dehart, D. B., Inagaki, T., Carson, J. L., Vrablic, T., Gesteland, K., and Schoenwolf, G. C. (1994). Morphogenesis of the murine node and notochordal plate. *Dev. Dyn.* 201, 260–278.
- Vogt, W. (1929). Gestaltungsanalyse am Amphibienkeim mit örtlicher Vitalfärbung. II. Teil. Gastrulation und mesodermbildung bei Urodelen und Anuren. *Wilhelm Roux’ Entwicklungsmech. Org.* 120, 384–706.
- Winklbauer, R. (1988). Differential interaction of *Xenopus* embryonic cells with fibronectin in vitro. *Dev. Biol.* 130, 175–183.
- Wintrebert, P. (1930). Analyse du développement de *Discoglossus pictus* Otth. par le procédé des marques colorées. La position dans l’oeuf des territoires invaginés. *C. R. Séances Soc. Biol.* 104, 1234–1238.

Received for publication August 3, 1995

Accepted December 8, 1995